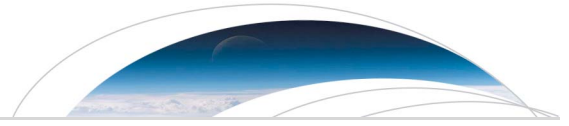




Originally published as:

Heit, B., Mancilla, F. d. L., Yuan, X., Morales, J., Sticks, D., Martin, R., Molina-Aguilera, A. (2017): Tearing of the mantle lithosphere along the intermediate-depth seismicity zone beneath the Gibraltar Arc: The onset of lithospheric delamination. - *Geophysical Research Letters*, 44, 9, pp. 4027—4035.

DOI: <http://doi.org/10.1002/2017GL073358>



## RESEARCH LETTER

10.1002/2017GL073358

## Key Points:

- Analysis of *S* receiver functions using data from a dense seismic profile across the Sierra Nevada Cordillera, southern Spain
- Detection of a 30 km step of the mantle lithosphere beneath the northern branch of the intermediate-depth seismic zone
- Implication of tearing in the mantle lithosphere that has propagated along the entire length of the intermediate-depth seismic zone

## Supporting Information:

- Supporting Information S1

## Correspondence to:

B. Heit,  
heit@gfz-potsdam.de

## Citation:

Heit, B., F. d. L. Mancilla, X. Yuan, J. Morales, D. Stich, Martín, R., and A. Molina-Aguilera (2017), Tearing of the mantle lithosphere along the intermediate-depth seismicity zone beneath the Gibraltar Arc: The onset of lithospheric delamination, *Geophys. Res. Lett.*, *44*, 4027–4035, doi:10.1002/2017GL073358.






Received 8 MAR 2017

Accepted 13 APR 2017

Accepted article online 19 APR 2017

Published online 4 MAY 2017

## Tearing of the mantle lithosphere along the intermediate-depth seismicity zone beneath the Gibraltar Arc: The onset of lithospheric delamination

Benjamin Heit<sup>1</sup> , Flor de Lis Mancilla<sup>2,3</sup>, Xiaohui Yuan<sup>1</sup> , Jose Morales<sup>2,3</sup> , Daniel Stich<sup>2,3</sup> , Rosa Martín<sup>2</sup> , and Antonio Molina-Aguilera<sup>2,3</sup>

<sup>1</sup>Deutsches GeoForschungsZentrum GFZ, Potsdam, Germany, <sup>2</sup>Instituto Andaluz de Geofísica, Universidad de Granada, Granada, Spain, <sup>3</sup>Departamento de Física Teórica y del Cosmos, Universidad de Granada, Granada, Spain

**Abstract** The intermediate-depth seismicity (IDS) beneath the Gibraltar Arc is enigmatic. So far, there is no general consensus on its relationship with the ongoing tectonic processes. We analyzed *S* wave receiver functions (SRFs) with data recorded by a dense N-S seismic profile deployed across the Sierra Nevada in southern Spain. SRF piercing points at depths of the lithosphere-asthenosphere boundary (LAB) sample an area of the IDS zone, providing an ideal opportunity to study the lithospheric structure at the IDS zone. We observe an abrupt change in the LAB depth along a profile from north to south across the northern branch of the IDS. The LAB depth changes from 90 to 100 km north of the IDS to ~130 km south of it. We propose that the IDS marks a tear in the Iberian mantle lithosphere along its entire length, implying an ongoing lithospheric delamination process that produces the seismicity at its onset.

### 1. Introduction

The Gibraltar Arc represents a complex plate boundary system at the western end of the Mediterranean Sea bounded by the converging Eurasian and African plates. It includes the Betics Cordillera in southern Iberia and the Rif mountains in Morocco and encloses the Neogene extensional Alboran Basin in between (Figure 1a). The plate boundary lies at the transition between the oceanic (Atlantic) to continental (Alboran Basin) domain, beneath which, a narrow subducted slab is descending from west to east to the deep mantle [e.g., *Gutscher et al.*, 2012]. The Gibraltar Arc is the result of ongoing convergence between Iberia and Africa, which currently has an oblique convergence in the NW-SE direction at a rate of 4–6 mm/yr [*Koulali et al.*, 2011]. The plate convergence began in the Cretaceous [*Dewey et al.*, 1988] and slowed down at ~25 Ma, accompanied by trench retreat and slab rollback, resulting in back-arc extension of the Alboran Sea [*Faccenna et al.*, 2004]. The accurate geometry of the plate boundary, as well as the mode of convergence, is not yet consistently constrained, resulting in a variety of tectonic models for this region [e.g., *Faccenna et al.*, 2004; *Vergés and Fernàndez*, 2012; *Platt et al.*, 2013; *Chertova et al.*, 2014].

Hypotheses involving either lithospheric delamination or slab detachment are used to explain the different tectonic models beneath the Gibraltar Arc. The convective removal model [*Platt and Vissers*, 1989], the pure delamination model [*Seber et al.*, 1996], and the slab subduction and rollback [*Loneragan and White*, 1997] are among the most widely accepted. All these models are able to produce asthenospheric influx in the upper mantle and generate fold-thrust belts and the development of extensional basins.

Recent tomographic studies [*Gutscher et al.*, 2002; *Spakman and Wortel*, 2004; *Bezada et al.*, 2013; *Villaseñor et al.*, 2015; *Palomeras et al.*, 2014] observed narrow high-velocity anomalies beneath the Gibraltar Arc and interpreted them as subducted mantle lithosphere sinking near vertically from west to east down to the mantle transition zone. Geodynamic modeling suggests that the present-day narrow slab geometry is resulted from a continuously southward and westward rollback since 35 Myr ago [*Chertova et al.*, 2014]. However, the shallow part of the slab is poorly resolved by the teleseismic tomography and the link of the slab to the deep seismicity is, so far, still unclear.

Continuous plate convergence has resulted in strong deformation within the crust and mantle lithosphere beneath the Gibraltar Arc, characterized by intensive seismicity. Crustal earthquakes are well distributed over the entire plate boundary region with concentration in the Betic-Rif Cordilleras, in the Alboran Sea along the Trans-Alboran Shear Zone (TASZ), and in the Gulf of Cadiz (Figure 1a). Beneath central western Betic and Alboran Sea, significant intermediate-depth seismicity (IDS) occurs in an intracontinental setting with

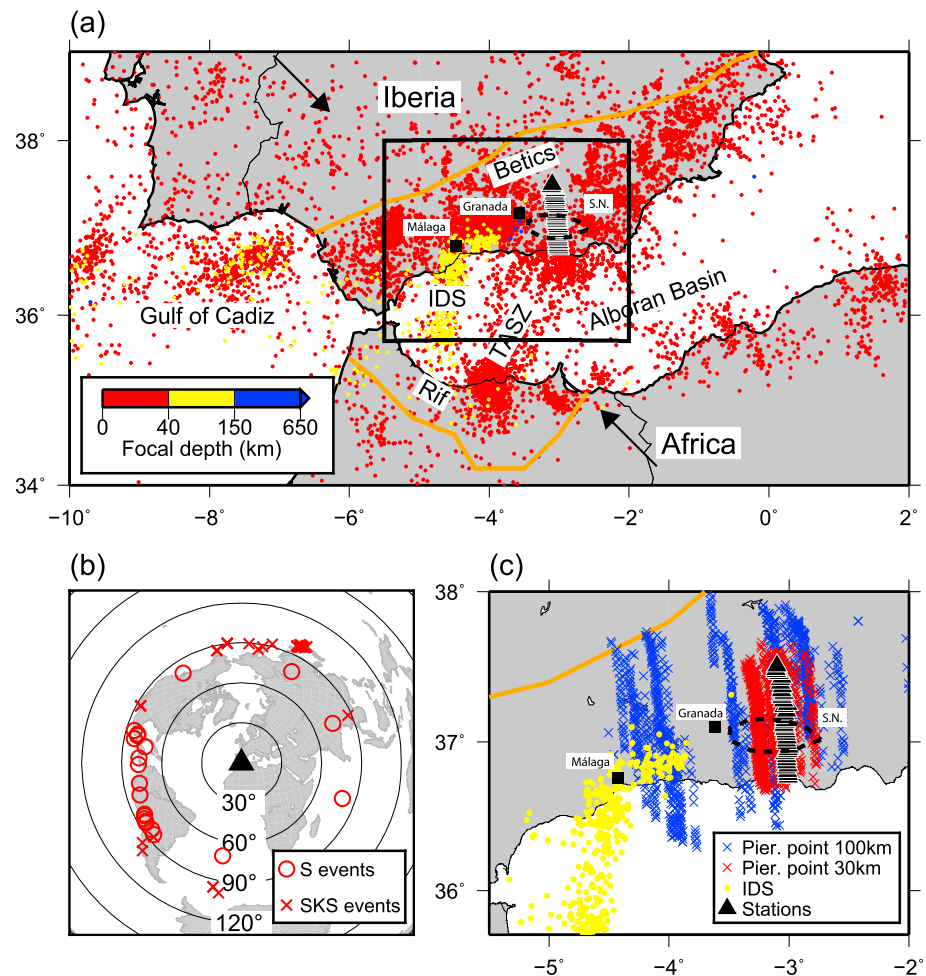


**Figure 1.** (a) Map of the Gibraltar Arc and the surroundings with simplified tectonic units including the Iberian Massif, the Betics-Rif Cordilleras and the Alboran Basin. The arrows represent relative plate motion after *Vernant et al.* [2010] and *Koulali et al.* [2011]. The Betics-Rif is part of an arcuate orogen revealing the complexity of this orogenic system that developed to the north and south of the Alboran Basin. Shallower seismicity with depth < 40 km is indicated as red circles. The intermediate-depth seismicity (earthquakes from the NEIC catalog between 40 km and 150 km) is shown as yellow circles. Seismic stations of the HIRE array are denoted by black triangles. The study area is highlighted by a black square. Dashed black line is the approximate position of the Sierra Nevada (S.N.). (b) Map of teleseismic earthquakes used in this study. The center of the HIRE profile is marked as a black triangle. Red circles denote earthquakes at epicentral distances between 60° and 85° used for S; red crosses are earthquakes for SKS phases between 85° and 115°. Black concentric circles are epicentral distances every 30°. (c) Map of stations (black triangles) and SRF piercing points at depths of 30 (red crosses) and 100 km (blue crosses). Dashed black line approximate position of the Sierra Nevada (S.N.). Yellow circles are intermediate-depth earthquakes at depths of 40–150 km.

earthquake focal depth ranging from ~50 to ~120 km beneath the western Alboran Sea [*Bufo* *et al.*, 1991; *Ruiz-Constán et al.*, 2011]. The IDS is focused along a narrow elongated zone with no detectable linear trend in focal depth distribution. The narrow IDS zone can be divided into two branches. The southern branch lies beneath the Alboran Sea and has an approximate north-south direction that turns to the east along the northern branch beneath the coastal area of the Betics Mountains (Figures 1a and 1c). The direction of the northern branch is toward the deep-focused earthquakes close to city of Granada (with depths greater than 620 km [*Chung and Kanamori*, 1976; *Bufo* *et al.*, 1991, 2004]), with a seismic gap between 120 and 620 km. Focal mechanisms of the IDS are dominated by dip slip with variable azimuthal orientation for larger earthquakes [*Mancilla et al.*, 2013], while they are highly heterogeneous for smaller earthquakes [*Martín et al.*, 2015] which complicate our understanding of the IDS. The seismicity has often been associated with high-velocity anomalies observed by seismic tomography [e.g., *Bezada et al.*, 2013; *Villaseñor et al.*, 2015] and was proposed to depict the geometry of the descending subducted slab

[Ruiz-Constán *et al.*, 2011]. However, homogeneous depth distribution along the IDS zone and the diversity of source mechanisms in the region provide arguments against this hypothesis. So far, it is unclear how the IDS is related to the subducted slab.

Detailed seismic images at the IDS region with high resolution are necessary to address this debating issue. Because there are nearly no seismic stations above the IDS in the Alboran Sea, seismic tomography has limited resolution at these depths and *P* wave receiver functions (PRFs) do not sample regions far away from stations. In contrast, *S* wave receiver functions (SRFs) can sample regions of the mantle lithosphere located farther away from the stations, because raypaths of *S*-to-*P* converted waves are much gentler than those of *P*-to-*S* conversions [Yuan *et al.*, 2006]. In this study, we apply the *S* receiver function (SRF) technique to study the structure of the mantle lithosphere and to map the lithosphere-asthenosphere boundary (LAB) across the IDS zone. Recording from teleseismic earthquakes were collected by a dense N-S trending array deployed across the Sierra Nevada in southern Spain.

## 2. Data and Methodology

The experiment of “high-resolution” receiver functions (HIRE) was operated for more than 1 year from the end of 2010 to the end of 2011. A total number of 40 broadband stations were deployed along a N-S linear array, stretching 80 km long from the south at the Mediterranean coast toward the north across all structural units of the Sierra Nevada (Figure 1a). Previous receiver function studies revealed strong lateral variations in the crust and uppermost mantle [Mancilla *et al.*, 2013, 2015a, 2015b]. The dense station spacing of ~2 km is appropriate for high-resolution imaging of the crust and mantle lithosphere by multifold RF stacking. Piercing points of the *S*-to-*P* conversions at the depth of the LAB provide dense sampling of the area across the northern branch of the IDS zone (Figure 1c).

The dominant wave period of the SRF is longer than 4 s, corresponding to a wavelength of >20 km. Therefore, the SRF cannot resolve fine crustal structures as in the case of *P* receiver functions (PRF). Mancilla *et al.* [2015a, 2015b, 2016] studied the detailed crustal structure using the *P*-to-*S* converted phases and mapped the Moho topography along the profile. The PRF is usually unable to provide useful images of the LAB in the depth range of 100–200 km as these depths are often affected by the Moho multiples and other crustal reverberations. In this work, we focus on the structure of the mantle lithosphere and display only images of the LAB by SRF. The main difference between PRF and SRF is that SRF are free of multiples that can mask the position of phases like the LAB located at certain depths. The reason behind this is related to the *P*-to-*S* converted phases arriving after the *P* wave, whereas *S*-to-*P* phases arrive before the *S*. This means that an *S*-to-*P* conversion have opposite time dependence compared to the *P*-to-*S* conversion. Being free of multiples, the SRF method is well suited to observe the LAB. However, due to interference with some other phases and the existence of overcritical incidence, the quality and quantity of the useful SRF data may be more limited compared to the PRF [e.g., Yuan *et al.*, 2006; Kind *et al.*, 2012].

Earthquakes with magnitudes (*m<sub>b</sub>*) greater than 5.5 at epicentral distances between 60° and 85° are used for the *S* phase and between 85° and 115° for the *SKS* phase to determine SRF (Figure 1b). Most of the events have back azimuths in the west and north; therefore, the SRF is only able to sample an area located west of the stations. The SRF analysis was performed using the approach of Kumar *et al.* [2005] and Yuan *et al.* [2006] (see also the supporting information). Waveform data have been visually inspected and manually selected according to signal/noise ratios. Coordinate rotation and deconvolution were performed to calculate the SRF. An additional step in the SRF processing is to reverse the time axis and to change the sign of amplitudes, so that the SRF from this work can be directly compared with the PRF retrieved for the same data set by Mancilla *et al.* [2015a, 2015b, 2016]. We obtained about 1300 *S* receiver functions.

We focus on the depth of the LAB to shed light on the structure of the lithosphere in the Alboran region. SRF piercing points at 100 km depth (assumed to be the approximate depth of the LAB in this region) sample the northern branch of the IDS zone (Figure 1c). We used a single scatterer approach [Kind *et al.*, 2002] to migrate the SRF. *S*-to-*P* converted amplitudes are backprojected to the space along the corresponding raypaths within a width of a Fresnel's zone. A 10 km × 20 km smoothing window is applied over the migration sections. Raypaths are estimated using the global 1-D velocity model IASP91 [Kennett and Engdahl, 1991].

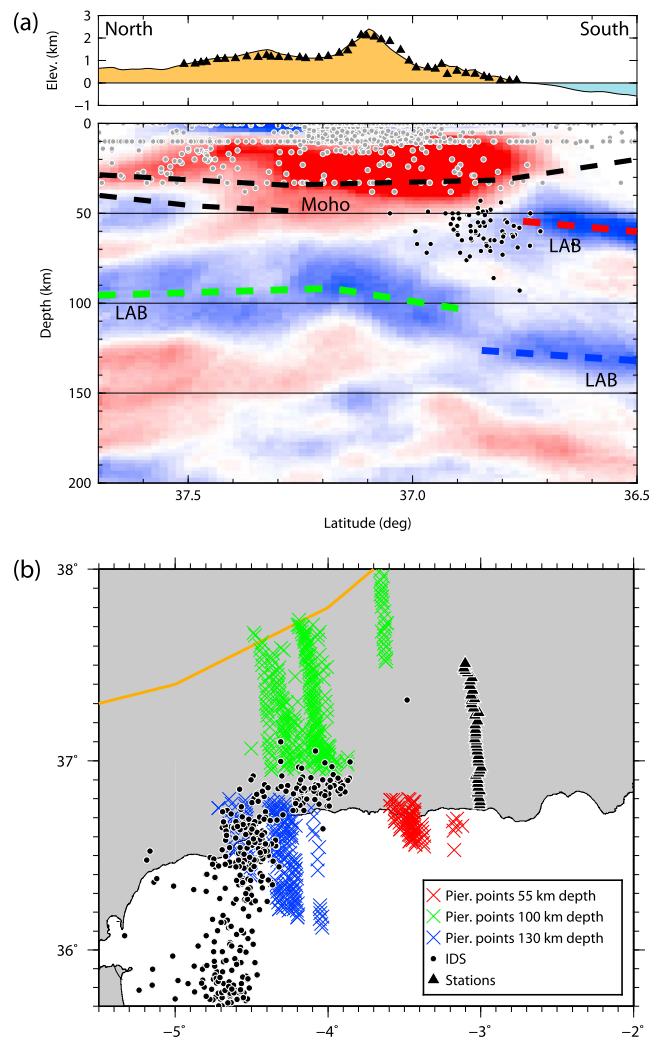


**Figure 2.** (a) Top: topography of along the seismic array and locations of the stations (black triangles). Bottom: migrated SRF cross section. Positive and negative amplitudes are denoted by red and blue colors, respectively. Gray and black circles denote crustal and intermediate-depth earthquakes, respectively, along the profile. Black dashed lines mark the Moho determined by PRF [Mancilla *et al.*, 2015a, 2015b, 2016]. Green, blue, and red dashed lines mark the Iberian and Alboran LAB at depths of 100 and 130, and 55 km, respectively. (b) Map of piercing points of the three LAB segments shown in Figure 2a.

down to a maximum depth of ~50 km. Discrepancy of Moho conversions between PRF and SRF exist north of 37.5°N, which could be explained by lateral variations due to different sampling areas of PRF and SRF, possible interference of crustal structures, or presence of noise.

A couple of significant negative conversions can be identified below the Moho in the depth range from 50 to 130 km. From north to south, a low-velocity phase at 90–100 km depth can be followed to about 36.9°N (marked as green dashed line in Figure 2a) and jumps to a depth of 130 km (blue dashed line in Figure 2a). At a shallower depth of ~55 km, another negative conversion is observed (red dashed line in Figure 2a), which seems to be absent north of 36.9°N. We interpret these negative conversions as the LAB of Alboran and Iberian domains, respectively. The changes in the LAB depth correlate well with the location of the IDS, spatially distributed below the coast, with higher concentration of seismicity between 40 and 100 km depth. The two southern LAB segments appear to dip slightly to the south. In Figure 2b we marked the locations of these three LAB segments, where they are observed (i.e., the SRF piercing points). The two deeper LAB segments

### 3. Results

We present the migrated SRF section in Figure 2a. The profile incorporates data with *S-to-P* conversion piercing points available within a 200 km wide swath that mainly samples the western region of the seismic array and down to a depth of 200 km (Figure 1c). Positive amplitudes dominate the depth range shallower than 50 km and are interpreted as the *S-to-P* conversions from the Moho, as well as, conversions from intracrustal discontinuities. Piercing points of the *S-to-P* conversions at the Moho depth (30–40 km) are close to the seismic stations, within a distance of ~30 km. Because of the long dominant wavelength (20 km) of the SRF and the complicated crustal structures along the profile, the SRF cannot reproduce a clear Moho conversion beneath Sierra Nevada and the adjacent basin areas with complicated crustal structures. We mark the Moho depth obtained by the PRF method [Mancilla *et al.*, 2016] on the SRF image as a reference and find an overall good agreement between both results. The Alboran Moho is located at shallow depths (~25 km) in the south at the Mediterranean coast and slightly deepens beneath the Betics to ~30 km depth. In the north (north of 37°N), the positive Moho phase in Figure 2a shows a thickening at this position on the SRF where the crust becomes thicker on the PRF (black dashed lines). This is also in agreement with the interpretation by Mancilla *et al.* [2015a, 2015b, 2016] suggesting that the Iberian crust is underthrusting the Alboran crust, extending

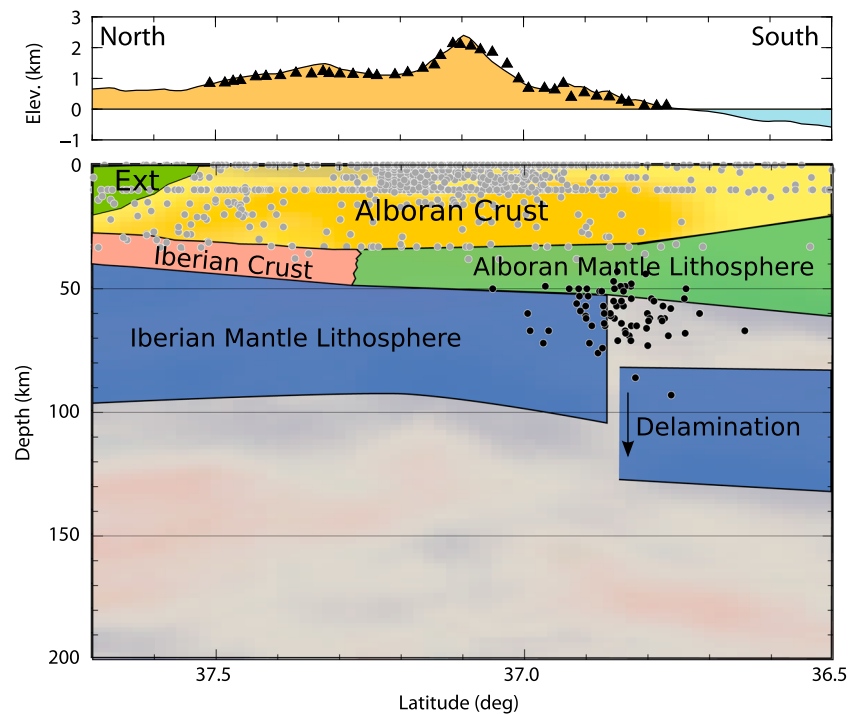


**Figure 3.** Interpretative drawing of the results from Figure 2a showing the real data in the background with interpretation in the front. The Alboran crust is shown as yellow. Ext.: External Betics and Iberian crust from *Mancilla et al.* [2015a]. Below the crust, the blue layer represents the Iberian mantle lithosphere underthrusting the Alboran crust with a breakoff in the southern part of the profile. The jump observed in velocities south of 36.9°N correlates well with the intermediate-depth seismicity. The Alboran mantle lithosphere is denoted by green.

are located west of 4°W, with the break exactly occurring at the place of the IDS. The shallower LAB segment is located farther east at ~3.5°W beneath the Alboran Basin. Raypath coverage (supporting information Figure S1b) shows that the northern half of the cross section is better sampled than the southern half, because most of the events come from the north and northwest. Nevertheless, the LAB is also well observed in the southern part of the profile due to large section width used. There is no data gap at the place of the LAB step. Note that a sharp change in the LAB depth may become smeared by long wavelength (>20 km) SRF. Lateral variations in the LAB depth are expected in our study area; however, they are not clearly revealed by our data with sufficient resolution. In supporting information Figure S2 we divided the entire data set in two cross sections with a width of 100 km. Although general variation in the LAB can be confirmed in both sections, more scatters can be seen in the western section, which can be partly attributed to the lower path density.

#### 4. Discussion

We interpret the two lower segments of LAB as the base of the Iberian mantle lithosphere and the upper LAB segment as the base of the Alboran mantle lithosphere (Figure 3). Beneath the Betic mountain belt, the Iberian LAB is located at a depth of 90–100 km and deepens slightly to the south until ~36.9°N, where the northern branch of the IDS is located. The depth of the Iberian LAB and southward deepening coincides well with depth values obtained by Rayleigh wave studies [*Palomeras et al.*, 2014]. Below the IDS and toward the south, our dense station deployment resolves an abrupt jump in the LAB to a greater depth of ~130 km. We propose that the step in the LAB depth at ~36.9°N is caused by a tear or breakoff in the Iberian lithosphere. The coincidence of the lithospheric tear with the IDS suggests that the seismicity might be related to a lithospheric breakoff. Southeast of the IDS zone, the base of the Alboran mantle lithosphere can be observed at a much shallower depth of 55 km, above the delaminated Iberian lithosphere.

*Mancilla et al.* [2013, 2015a, 2015b] mapped the Moho beneath our study area and observed underthrusting of the Iberian crust beneath the Alboran crust. At the place of the IDS, the underthrusting Iberian crust has

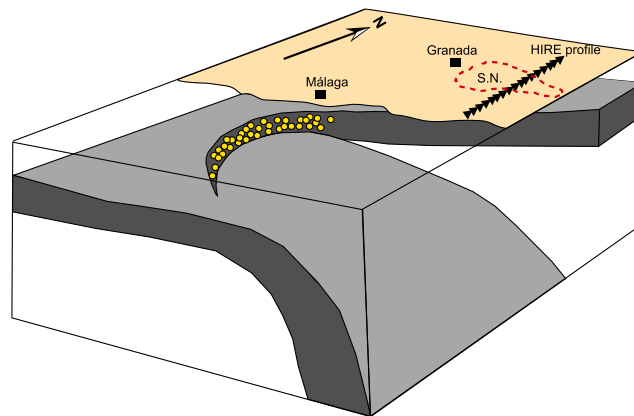


**Figure 4.** Three-dimensional cartoon showing the slab breakoff driven by slab pull and rollback, inducing the intermediate-depth seismicity (IDS) (yellow circles) beneath Malaga and the western Alboran Sea. Inverted triangles resemble the stations location along the HIRE profile. Red dashed line represents the approximate location of the Sierra Nevada (S.N.). The IDS occurs along the rupture of the detached lithosphere. The Alboran lithosphere is not shown here.

in the northern branch of the IDS (near the coast) with maximum focal depths of 100 km. On the contrary, an alignment of the IDS along a SE dipping, planar subduction interface, as proposed by *Ruiz-Constán et al.* [2011], is not evident and not supported by our results. The IDS follows a roughly horizontal lineament or escarpment, possibly in a vertical rupture interface. Vertical dip slip mechanisms inferred from moment tensor inversion for the larger earthquakes within the IDS are in agreement with a lithospheric breakoff in the vertical direction and support this model [*Mancilla et al.*, 2013].

The simplified cartoon in Figure 4 shows the main results and our interpretation. Across the northern portion of the IDS, trending E-W beneath the continent, we observe a tear in the mantle lithosphere. We propose that the tearing is propagating toward the south along the entire IDS zone. The location of the IDS marks the onset of lithospheric detachment. Furthermore, the IDS terminates at  $\sim 3.9^\circ\text{W}$ , east of which the lithosphere is completely detached. This idea was already postulated by *Mancilla et al.* [2015b] and presented as a cartoon where it is possible to observe an incipient delamination propagating toward the west that ends at the position of the city of Malaga on the surface. With our results, we are able to follow this structure farther toward the southwest and to establish a correlation between the delamination and the onset of intermediate-depth earthquakes. With the current resolution of seismic tomography [*Gutscher et al.*, 2002; *Bezada et al.*, 2013; *Villaseñor et al.*, 2015], the spatial relationship between a remnant Alboran slab of oceanic origin with delaminated continental lithosphere and the IDS remains speculative. Our results are supported by *Palomeras et al.* [2014] shear wave tomographic results suggesting that the IDS under the Betics is possibly related to the slab in the process of detachment. *Thurner et al.* [2014] using receiver functions have found similar evidence and also suggested that the slab remains attached to the base of the continental lithosphere in the area north of the IDS where we observe no detachment. The IDS coincides roughly with the high-velocity bodies seen by seismic tomography [e.g., *Villaseñor et al.*, 2015], which supports our interpretation. In fact, a slab breakoff was also suggested by *Villaseñor et al.* [2015]. Our observation of the lithospheric tear along the IDS provides new evidence of the mechanism that gives origin to the earthquakes of the IDS zone beneath the Gibraltar Arc. Due to subduction retreat and slab rollback [e.g., *Lonergan and White*, 1997], the subducted slab is bending toward the west at a near-vertical position [e.g., *Villaseñor et al.*, 2015] and is pulling down by gravitational force, producing a slab breakoff at the depth of maximum bending and weakness represented by the seismicity observed at the IDS.

Two competing groups of models are mainly used to explain the tectonic evolution of the Gibraltar Arc: delamination/convective removal of continental lithosphere [e.g., *Calvert et al.*, 2000; *Platt et al.*, 2013] or active oceanic subduction [e.g., *Gutscher et al.*, 2012; *Villaseñor et al.*, 2015]. All proposed models involve a cold, negatively buoyant lithosphere sinking into the deep mantle; however, they debate on whether the sinking lithosphere is oceanic or continental and how it is connected to the remaining

detached from the Alboran crust and delaminated into the mantle. These images indicate tearing of the underthrust crust beneath southeast Spain, which led to the prediction of slab rupture beneath the IDS zone, although the latter is located outside the coverage from PRF piercing points [*Mancilla et al.*, 2015a, 2015b]. Our observation of the LAB step beneath the IDS supports this hypothesis. Furthermore, we propose that the lithospheric tearing is representing an ongoing process that would eventually rupture the entire length of the IDS zone beneath the Alboran Sea. Relocation of the IDS [*Santos Bueno*, 2016] suggests that most of the earthquakes are concentrated in a zone less than 25 km wide

lithosphere. Among the processes that are responsible for reworking and recycling of lithospheric material into the mantle are the piecemeal removal or delamination and the subduction of oceanic lithosphere. Lithospheric delamination is associated with continental collision regimes and was introduced by *Bird* [1979] to explain lithospheric foundering observed in the Colorado Plateau. Convective removal associated with dense and unstable mantle material being removed and driven into the asthenosphere was proposed by *Houseman et al.* [1981]. Both terms are usually not differentiated in the literature [*Ducea*, 2011] and are used to refer the same type of process implying the recycling of lithospheric material. On the other hand, the term subduction implies that when two plates converge, the denser one (oceanic lithosphere) will sink into the mantle in a process that is driven by the convergence rate. At the late stage of the subduction when the oceanic plate has been completely consumed, the buoyant continental lithosphere that is attached to the subducted plate could continue to subduct due to processes of slab pull and rollback. At the final stage, the descending slab will detach from the upper part due to buoyancy of continental lithosphere.

The idea of delamination and lithospheric removal has been used in the Alboran region to explain the absence of correlation between thick crust and high topography in the Betics [*Mancilla et al.*, 2013, 2015a, 2015b] or the origin of deep earthquakes beneath Granada as produced by detached material from the slab [e.g., *Calvert et al.*, 2000] and seen as high-velocity anomalies at depths of ~600 km. We speculate that a combination of delamination and piecemeal removal of lithosphere would accompany the slab retreat induced by slab rollback (i.e., enforced by slab pull) following the cease of subduction. The slab rollback, therefore, may be responsible for changes in the tectonic regime from compression to extension in the Alboran convergent setting as suggested by other authors [e.g., *Lonergan and White*, 1997].

Furthermore, our observations suggest a tear in the descending mantle lithosphere along the IDS, which implies a scenario of the final stage of the subduction. At this stage, delamination and subduction would refer to the same dynamic model. The complete breakoff and detachment of the slab should mark the termination of the Gibraltar subduction.

Ongoing delamination beneath the Alboran Sea leaves its signature at crustal levels through extension in the central Betics and a distinct anomaly in the direction and magnitude of GPS velocities across southern Spain [e.g., *Mancilla et al.*, 2013; *Palano et al.*, 2015]. The position of the deeper LAB phase inferred in this study and the intermediate-depth seismicity coincides with these results, as well as with the high topography of the Sierra Nevada block. This would suggest that there is an intrinsic correlation between the lithospheric detachment and uplift in this region. The detachment process could have triggered the uplift of the western border of the Sierra Nevada producing a great number of earthquakes in response to the ongoing foundering of the lithosphere. A similar idea has been suggested by *Azañón et al.* [2012] as they found that the uplift of the Sierra Nevada on the western side was accompanied by subsidence of the Granada Basin and uplift of the Gaudix Basin during the Quaternary. The uplift of Sierra Nevada is evidenced in the west, where the highest topography is located and hence might correlate well with asthenospheric influx due to ongoing delamination at the position where we detected the jump in the depth of the LAB.

## 5. Conclusions

S receiver functions reveal a step in the LAB depth along the northern branch of the IDS zone near the Gibraltar Arc in the western Alboran Sea, which we interpret as mantle lithospheric breakoff. We propose that the lithospheric tearing has further migrated to the south along the entire length of the IDS zone and suggest that the rupture along the IDS marks the onset of the lithospheric delamination. The steeply subducted slab is breaking off at this place, probably marking the termination of the Gibraltar subduction. The breakoff as a result of slab pull and rollback is the natural explanation for the ongoing delamination and the existence of intermediate-depth seismicity in this region. We postulate that the slab breakoff at the position of the IDS is an ongoing process that might be responsible for future earthquakes in this region as the slab rolls back and tears down the upper portion of the lithosphere. With this data, we are able to show that there is a correlation between slab detachment and local intermediate-depth seismicity. Finally, our explanation is in agreement with different geophysical models proposed to shed light in this geodynamically complicated region.



### Acknowledgments

The experiment was supported by Deutsches GeoForschungsZentrum (GFZ) and Instituto Andaluz de Geofísica (IAG), Universidad de Granada. The project "Imagen 3D de la estructura litosférica y del manto superior de la Península Ibérica y norte de Marruecos: hacia un nuevo modelo geodinámico" is funded by the University of Granada. Additional funding is provided by project CGL2015-67130-C2-2-R. Equipment was provided by Geophysical Instrument Pool Potsdam (GIPP). Continuous waveform data of the HIRE network (9C) are archived at the GEOFON data center [Heit et al., 2010]. We are grateful to many colleagues from the GFZ and IAG, who took part in the field experiments. We also thank R. Kind for promoting and supporting the deployment of dense seismic arrays in the Sierra Nevada region.

### References

- Azañón, J. M., J. V. Pérez-Peña, F. Giacomia, G. Booth-Rea, J. M. Martínez-Martínez, and M. J. Rodríguez-Peces (2012), Active tectonics in the central and eastern Betic Cordillera through morphotectonic analysis: The case of Sierra Nevada and Sierra Alhamilla, *J. Iber. Geol.*, *38*(1), 225–238.
- Bezada, M. J., E. D. Humphreys, D. R. Toomey, M. Harnafi, J. M. Davila, and J. Gallart (2013), Evidence for slab rollback in westernmost Mediterranean from improved upper mantle imaging, *Earth Planet. Sci. Lett.*, *368*, 51–60.
- Bird, P. (1979), Continental delamination and the Colorado Plateau, *J. Geophys. Res.*, *84*, 7561–7571, doi:10.1029/JB084iB13p07561.
- Bufo, E., A. Udias, and R. Madariaga (1991), Intermediate and deep earthquakes in Spain, *Pure Appl. Geophys.*, *136*, 375–393.
- Bufo, E., M. Bezzeghoud, A. Udias, and C. Pro (2004), Seismic sources on the Iberia-African plate boundary and their tectonic implications, *Pure Appl. Geophys.*, *161*, 623–646.
- Calvert, A., E. Sandvol, D. Seber, M. Barazangi, S. Roecker, T. Mourabit, F. Vidal, G. Alguacil, and N. Jabour (2000), Geodynamic evolution of the lithosphere and upper mantle beneath the Alboran region of the western Mediterranean: Constraints from travel time tomography, *J. Geophys. Res.*, *105*, 10,871–10,898, doi:10.1029/2000JB900024.
- Chertova, M. V., W. Spakman, T. Geenen, A. P. van den Berg, and D. J. J. van Hinsbergen (2014), Underpinning tectonic reconstructions of the western Mediterranean region with dynamic slab evolution from 3-D numerical modeling, *J. Geophys. Res. Solid Earth*, *119*, 5876–5902, doi:10.1002/2014JB011150.
- Chung, W. Y., and H. Kanamori (1976), Source process and tectonic implications of the Spanish deep-focus earthquake of March 29, 1954, *Phys. Earth Planet. Inter.*, *13*, 85–96.
- Dewey, J. F., M. L. Helman, E. Turco, D. H. W. Hutton, and S. D. Knott (1988), Kinematics of the western Mediterranean, *Geol. Soc. London Spec. Publ.*, *45*, 265–283.
- Ducea, M. (2011), Fingerprinting orogenic delamination, *Geology*, *39*, 191–192.
- Faccenna, C., C. Piromallo, A. Crespo-Blanc, L. Jolivet, and F. Rossetti (2004), Lateral slab deformation and the origin of the western Mediterranean arcs, *Tectonics*, *23*, TC1012, doi:10.1029/2002TC001488.
- Gutscher, M.-A., J. A. Malod, J.-P. Rehault, I. Contrucci, F. Klingelhoefer, L. Mendes-Victor, and W. Spakman (2002), Evidence for active subduction beneath Gibraltar, *Geology*, *30*, 1071–1074.
- Gutscher, M.-A., et al. (2012), The Gibraltar subduction: A decade of new geophysical data, *Tectonophysics*, *574–575*, 72–91.
- Heit, B., X. Yuan, and F. Mancilla (2010), High resolution seismological profiling across Sierra Nevada (HIRE), Deutsches GeoForschungsZentrum GFZ. Other/Seismic Network, doi:10.14470/4P7565788335.
- Houseman, G.A., D. P. McKenzie, and P. Molnar (1981), Convective instability of a thickened boundary-layer and its relevance for the Thermal evolution of continental convergent belts, *J. Geophys. Res.*, *86*, 6115–6132, doi:10.1029/JB086iB07p06115.
- Kennett, B. L. N., and E. R. Engdahl (1991), Traveltimes for global earthquake location and phase identification, *Geophys. J. Int.*, *105*, 429–465.
- Kind, R., et al. (2002), Seismic images of crust and upper mantle beneath Tibet: Evidence for Eurasian plate subduction, *Science*, *298*, 1219–1221.
- Kind, R., X. Yuan, and P. Kumar (2012), Seismic receiver functions and the lithosphere–asthenosphere boundary, *Tectonophysics*, *536–537*, 25–43, doi:10.1016/j.tecto.2012.03.005.
- Koulali, A., D. Ouazar, A. Tahayt, R. W. King, P. Vernant, R. E. Reilinger, S. Mc Clusky, T. Mourabit, J. M. Davila, and N. Amraoui (2011), New GPS constraints on active deformation along the Africa–Iberia plate boundary, *Earth Planet. Sci. Lett.*, *308*, 211–217.
- Kumar, P., X. Yuan, R. Kind, and G. Kosarev (2005), The lithosphere–asthenosphere boundary in the Tien Shan–Karakoram region from S receiver functions: Evidence for continental subduction, *Geophys. Res. Lett.*, *32*, L07305, doi:10.1029/2004GL022291.
- Lonergan, L., and N. White (1997), Origin of the Betic-Rif mountain belt, *Tectonics*, *16*, 504–522.
- Mancilla, F., D. Stich, M. Berrocoso, R. Martin, J. Morales, A. Fernández-Ros, R. Paez, and A. Pérez-Peña (2013), Delamination in the Betic Range: Deep structure, seismicity, and GPS motion, *Geology*, *41*, 307–310.
- Mancilla, F., G. Booth-Rea, D. Stich, J. V. Pérez-Peña, J. Morales, J. M. Azañón, R. Martin, and F. Giacomia (2015a), Slab rupture and delamination under the Betics and Rif constrained from receiver functions, *Tectonophysics*, *663*, 225–237.
- Mancilla, F., et al. (2015b), Crustal thickness and images of the lithospheric discontinuities in the Gibraltar arc and surrounding areas, *Geophys. J. Int.*, *203*(3), 1804–1820, doi:10.1093/gji/ggv390.
- Mancilla, F., A. Aguilera-Molina, B. Heit, J. Morales, X. Yuan, D. Stich, and R. Martin (2016), A sharp Moho step under central and eastern Betics, western Mediterranean region, paper presented at EGU General Assembly 2016, *Geophys. Res. Abstr.*, vol. 18, EGU2016-17265.
- Martin, R., D. Stich, J. Morales, F. Mancilla (2015), Moment tensor solutions for the Iberian-Maghreb region during the IberArray deployment (2009–2013), *Tectonophysics*, *663*, 261–274.
- Platt, J. P., and R. L. M. Vissers (1989), Extensional collapse of thickened continental lithosphere: A working hypothesis for the Alboran Sea and Gibraltar arc, *Geology*, *17*, 540–543.
- Palano, M., P. J. González, and J. Fernández (2015), The diffuse plate boundary of Nubia and Iberia in the western Mediterranean: Crustal deformation evidence for viscous coupling and fragmented lithosphere, *Earth Planet. Sci. Lett.*, *430*, 439–447, doi:10.1016/j.epsl.2015.08.040.
- Palomeras, I., S. Thurner, A. Levander, K. Liu, A. Villaseñor, R. Carbonell, and M. Harnafi (2014), Finite-frequency Rayleigh wave tomography of the western Mediterranean: Mapping its lithospheric structure, *Geochem. Geophys. Geosyst.*, *15*, 140–160, doi:10.1002/2013GC004861.
- Platt, J. P., W. M. Behr, K. Johannesen, and J. R. Williams (2013), The Betic-Rif Arc and its Orogenic Hinterland: A review, *Annu. Rev. Earth Planet. Sci.*, *41*, 313–57.
- Ruiz-Constán, A., J. Galindo-Zaldívar, A. Pedrera, B. Célérier, and C. Marín-Lechado (2011), Stress distribution at the transition from subduction to continental collision (northwestern and central Betic Cordillera), *Geochem. Geophys. Geosyst.*, *12*, Q12002, doi:10.1029/2011GC003824.
- Santos Bueno, N. (2016), Localización de terremotos intermedios del Mar de Alborán durante el despliegue de redes temporales densas, Master thesis, Univ. of Granada, Spain. [Available at [http://masteres.ugr.es/geomet/pages/info\\_academica/tfm/20152016/nereasantosresumen](http://masteres.ugr.es/geomet/pages/info_academica/tfm/20152016/nereasantosresumen).]
- Seber, D., M. Barazangi, A. Ibenbrahim, and A. Demnati (1996), Geophysical evidence for lithospheric delamination beneath the Alboran Sea and Rif-Betic mountains, *Nature*, *379*, 785–790.
- Spakman, W., and R. Wortel (2004), A tomographic view on western Mediterranean geodynamics, in *The TRANSMED Atlas: The Mediterranean Region From Crust to Mantle*, edited by W. Cavazza et al., pp. 31–52, Springer, Berlin.
- Thurner, S., I. Palomeras, A. Levander, R. Carbonell, and C. T. Lee (2014), Ongoing lithospheric removal in the Western Mediterranean: Evidence from Ps receiver functions and thermobarometry of Neogene basalts (PICASSO project), *Geochem. Geophys. Geosyst.*, *15*, 1113–1127.

- Vergés, J., and M. Fernández (2012), Tethys–Atlantic interaction along the Iberia–Africa plate boundary: The Betic–Rif orogenic system, *Tectonophysics*, *579*, 144–172.
- Vernant, P., A. Fadil, T. Mourabit, D. Ouazar, A. Koulali, J. M. Davila, J. Garate, S. McClusky, and R. E. Reilinger (2010), Geodetic constraints on active tectonics of the western Mediterranean: Implications for the kinematics and dynamics of the Nubia–Eurasia plate boundary zone, *J. Geodyn.*, *49*, 123–129, doi:10.1016/j.jog.2009.10.007.
- Villaseñor, A., S. Chevrot, M. Harnafi, J. Gallart, A. Pazos, I. Serrano, D. Córdoba, J. A. Pulgar, and P. Ibarra (2015), Subduction and volcanism in the Iberia–North Africa collision zone from tomographic images of the upper mantle, *Tectonophysics*, *663*, 238–249.
- Yuan, X., R. Kind, X. Li, and R. Wang (2006), The *S* receiver functions: Synthetics and data example, *Geophys. J. Int.*, *165*, 555–564.